

Synergetic Regulator Synthesis for a Class of Nonlinear Systems

Nusawardhana* Jianming Lian[†] Mohamed Zribi[‡] Stanisław H. Żak[§]

June 8, 2011

Abstract

The integral action method combined with the synergetic control design approach are employed to synthesize regulators for a class of nonlinear dynamical systems. The integral action is commonly used in the design of controllers to track constant or almost constant reference signals. The proposed method offers a closed-form analytic solution. An attractive feature of the proposed approach is that the control law is obtained by solving the first-order differential equation. The stability analysis of the closed-loop system driven by the proposed regulator is performed and illustrated with two simulation examples: the regulator design for a wing-rock suppression problem and a two-link manipulator.

Keywords: Synergetic control, invariant manifold, output regulation, integral action

*Cummins, Inc., 1460 National Road, Columbus, IN 47201

[†]Center for Advanced Power Systems, Florida State University, 2000 Levy Street, Tallahassee, FL 32310

[‡]Electrical Engineering Department, Kuwait University, P.O. Box 5969, Safat 13060, Kuwait

[§]School of Electrical and Computer Engineering, Purdue University, 465 Northwestern Avenue, West Lafayette, IN 47907-2035

1 Introduction

An attractive feature of synergetic control is that solving the first-order differential equation provides a closed-form solution to the regulator problem. For an elementary introduction to the subject of synergetic control and its applications to power electronics, we recommend Refs. [1, 2, 3, 4]. In this paper, we combine a synergetic control approach with an integral action method in the regulator design. The integral action is commonly used in the design of controllers to track constant or almost constant reference signals [5].

The paper is organized as follows. In the following section, we present elements of synergetic control approach that we employ in this paper. Then, we apply the synergetic control approach to the synthesis of a regulator using the integral action. Stability analysis of the closed-loop system is performed, and an algorithm for the construction of a stable invariant manifold, an essential element of synergetic regulator design, is formulated. Finally, we test the proposed algorithm for the regulator construction to design regulators for a nonlinear wing-rock suppression problem and a two-link robotic manipulator.

2 Synergetic Control Method

Consider a class of nonlinear dynamical systems modeled as

$$\dot{\mathbf{x}} = \mathbf{f}(\mathbf{x}) + \mathbf{B}(\mathbf{x})\mathbf{u}, \quad (1)$$

where \mathbf{x} is a vector of state variables of dimension n , \mathbf{u} is the input vector of dimension m , $\mathbf{f}(\mathbf{x})$ is a state-dependent function of dimension n , $\mathbf{B}(\mathbf{x})$ is a state-dependent input function matrix of dimension $n \times m$ and it has full column rank everywhere.

Let $\boldsymbol{\sigma} = \mathbf{s}(\mathbf{x}) : \mathbb{R}^n \rightarrow \mathbb{R}^m$ be a vector function of dimension m .

The objective of the control problem, discussed in this paper, is to find a control policy that stabilizes the system (1) by steering the system (1) trajectories to a manifold,

$$\mathcal{M} = \{\mathbf{x} : \boldsymbol{\sigma} = \mathbf{0}\} \quad (2)$$

and force the trajectories to stay on the manifold thereafter.

We further require that, (i) the system (1) confined to the manifold $\mathcal{M} = \{\mathbf{x} : \boldsymbol{\sigma} = \mathbf{0}\}$ is asymptotically stable to the origin, (ii) $\boldsymbol{\sigma} = \mathbf{s}(\mathbf{x})$ is constructed so that the square $m \times m$ matrix $\mathbf{s}_{\mathbf{x}}(\mathbf{x})\mathbf{B}(\mathbf{x})$ is invertible, where $\mathbf{s}_{\mathbf{x}}$ is the Jacobian matrix of $\mathbf{s}(\mathbf{x})$ with respect to \mathbf{x} . It is shown in Refs. [3], [4] that when these two conditions are satisfied, the solution to the above control problem is obtained by solving the associated first-order ordinary differential equation

$$\mathbf{T}\dot{\boldsymbol{\sigma}} + \boldsymbol{\sigma} = \mathbf{0}, \quad (3)$$

where $\mathbf{T} \in \mathbb{R}^{m \times m}$ is a symmetric positive definite matrix. The control policy is the solution to the first-order differential equation (3), that is,

$$\begin{aligned} \mathbf{u} &= -(\mathbf{T}\mathbf{s}_{\mathbf{x}}(\mathbf{x})\mathbf{B}(\mathbf{x}))^{-1}(\mathbf{T}\mathbf{s}_{\mathbf{x}}(\mathbf{x})\mathbf{f}(\mathbf{x}) + \mathbf{s}(\mathbf{x})) \\ &= -(\mathbf{s}_{\mathbf{x}}(\mathbf{x})\mathbf{B}(\mathbf{x}))^{-1}\mathbf{s}_{\mathbf{x}}(\mathbf{x})\mathbf{f}(\mathbf{x}) - (\mathbf{s}_{\mathbf{x}}(\mathbf{x})\mathbf{B}(\mathbf{x}))^{-1}\mathbf{T}^{-1}\mathbf{s}(\mathbf{x}). \end{aligned} \quad (4)$$

The use of the control law (4) in the nonlinear dynamical systems (1) makes the invariant manifold $\mathcal{M} = \{\mathbf{x} : \boldsymbol{\sigma} = \mathbf{0}\}$ attractive. The control law (4) drives closed-loop trajectories of (1) from any initial condition towards the invariant manifold \mathcal{M} . As stated above, $\boldsymbol{\sigma}$ is constructed in such a way that all trajectories of (1) confined on \mathcal{M} converge to the origin. Therefore, the stability of the closed-loop trajectories is achieved in two modes: (i) closed-loop trajectories converging to the manifold $\mathcal{M} = \{\mathbf{x} : \boldsymbol{\sigma} = \mathbf{0}\}$, and (ii) closed-loop trajectories moving along the manifold $\mathcal{M} = \{\mathbf{x} : \boldsymbol{\sigma} = \mathbf{0}\}$ towards the origin.

The synergetic control design method employs the following two-step design procedure:

1. Construct an asymptotically stable invariant manifold $\mathcal{M} = \{\mathbf{x} : \boldsymbol{\sigma} = \mathbf{0}\}$, (i.e. all trajectories of the system confined to \mathcal{M} converge asymptotically to the origin).
2. Construct the controller \mathbf{u} using (4).

The synergetic control approach shares similarity with that of the variable structure sliding mode control (SMC). This relation was discussed in Refs. [1], [2], [3], [4]. It was observed in Refs. [3], [4] that the first term of the control policy (4) is the so-called ‘‘equivalent

control,” while the second term may be viewed as an “approximation to the discontinuous control law” of the SMC. Additionally, the method of constructing a stable invariant manifold proposed in [6] will be directly applied to the construction of the invariant manifold in this paper.

In the development of the proposed regulator, we adopt the integral tracking method used in the sliding mode tracking controller design described in Ref. [7]. The resulting controller drives the closed-loop dynamics so that the integral of the tracking error converges to zero. This is essentially a regulation problem of the “integral error” for which regulation methods using synergetic control [3, 4] can be applied.

3 System Description

The class of nonlinear systems that we consider is modeled by

$$\begin{aligned}\dot{\mathbf{x}} &= \mathbf{f}(\mathbf{x}) + \mathbf{B}(\mathbf{x})\mathbf{u} \\ &= \mathbf{A}(\mathbf{x})\mathbf{x} + \hat{\mathbf{B}}\tilde{\mathbf{u}}.\end{aligned}\tag{5}$$

We assume that the system (5) is transformable into the following “regular form” [8], [7],

$$\begin{bmatrix} \dot{\mathbf{x}}_1 \\ \dot{\mathbf{x}}_2 \end{bmatrix} = \begin{bmatrix} \mathbf{A}_{11} & \mathbf{A}_{12} \\ \mathbf{A}_{21}(\mathbf{x}) & \mathbf{A}_{22}(\mathbf{x}) \end{bmatrix} \begin{bmatrix} \mathbf{x}_1 \\ \mathbf{x}_2 \end{bmatrix} + \begin{bmatrix} \mathbf{O} \\ \mathbf{B}_u \end{bmatrix} \tilde{\mathbf{u}},\tag{6}$$

where the state vector \mathbf{x}_1 is in \mathbb{R}^{n-m} , the state vector \mathbf{x}_2 is in \mathbb{R}^m , and the control vector \mathbf{u} is in \mathbb{R}^m . The matrix $\mathbf{O} \in \mathbb{R}^{(n-m) \times m}$ is a matrix with zero entries. The matrix $\mathbf{B}_u \in \mathbb{R}^{m \times m}$ is invertible and the matrices \mathbf{A}_{ij} , $i = 1, 2$, $j = 1, 2$ have appropriate dimensions. Note that \mathbf{A}_{1j} ’s, $j = 1, 2$, are constant matrices, while \mathbf{A}_{2j} ’s, $j = 1, 2$, are state-dependent matrices. For a constructive algorithm that can be used to transform (5) into the regular form given by (6), we refer to Ref. [7, p. 66].

An example of physical systems that can be modeled using the above non-linear regular form are natural Lagrangian systems. A simple example of a natural Lagrangian system whose model can be represented in the regular form is a planar two-link robot. Indeed, let

$\mathbf{x}_1 = [\theta_1 \ \theta_2]^\top$ be the vector of joint angles, $\boldsymbol{\tau} = [\tau_1 \ \tau_2]^\top$ be the vector of torques applied to the joints. A detailed modeling of such a robot can be found in [9, p. 396], and its dynamics are given by

$$\mathbf{H}(\mathbf{x}_1)\ddot{\mathbf{x}}_1 + \mathbf{C}(\mathbf{x}_1, \dot{\mathbf{x}}_1)\dot{\mathbf{x}}_1 + \mathbf{g}(\mathbf{x}_1) = \boldsymbol{\tau}, \quad (7)$$

where $\mathbf{H}(\mathbf{x}_1)$ is the manipulator inertia matrix and $\mathbf{C}(\mathbf{x}_1, \dot{\mathbf{x}}_1)\dot{\mathbf{x}}_1$ is the vector of centripetal and Coriolis torques, and $\mathbf{g}(\mathbf{x}_1) = \begin{bmatrix} g_1(\mathbf{x}_1) & g_2(\mathbf{x}_1) \end{bmatrix}^\top$ is the vector of gravitational torques. Because the inertia matrix $\mathbf{H}(\mathbf{x}_1)$ is positive definite over the whole workspace, we know that $\mathbf{H}^{-1}(\mathbf{x}_1)$ exists and is also positive definite. Let

$$\mathbf{G}(\mathbf{x}_1) = \begin{bmatrix} \frac{g_1(\mathbf{x}_1)}{x_1} & 0 \\ 0 & \frac{g_2(\mathbf{x}_1)}{x_2} \end{bmatrix}.$$

Using the above we can represent the term $\mathbf{g}(\mathbf{x}_1)$ as

$$\mathbf{g}(\mathbf{x}_1) = \mathbf{G}(\mathbf{x}_1)\mathbf{x}_1. \quad (8)$$

Taking into account (8), we can rewrite (7) as

$$\ddot{\mathbf{x}}_1 = -\mathbf{H}^{-1}(\mathbf{x}_1)\mathbf{C}(\mathbf{x}_1, \dot{\mathbf{x}}_1)\dot{\mathbf{x}}_1 - \mathbf{H}^{-1}(\mathbf{x}_1)\mathbf{G}(\mathbf{x}_1)\mathbf{x}_1 + \mathbf{H}^{-1}(\mathbf{x}_1)\boldsymbol{\tau}. \quad (9)$$

Let $\mathbf{x}_2 = \dot{\mathbf{x}}_1$ and $\tilde{\mathbf{u}} = \mathbf{H}^{-1}(\mathbf{x}_1)\boldsymbol{\tau}$. Then, the dynamics of the planar two-link robot modeled by (9) can be represented in the form of (6), that is,

$$\begin{bmatrix} \dot{\mathbf{x}}_1 \\ \dot{\mathbf{x}}_2 \end{bmatrix} = \begin{bmatrix} \mathbf{O} & \mathbf{I}_2 \\ -\mathbf{H}^{-1}(\mathbf{x}_1)\mathbf{G}(\mathbf{x}_1) & -\mathbf{H}^{-1}(\mathbf{x}_1)\mathbf{C}(\mathbf{x}_1, \mathbf{x}_2) \end{bmatrix} \begin{bmatrix} \mathbf{x}_1 \\ \mathbf{x}_2 \end{bmatrix} + \begin{bmatrix} \mathbf{O} \\ \mathbf{I}_2 \end{bmatrix} \tilde{\mathbf{u}}. \quad (10)$$

4 Regulator Design

Suppose that the output $\mathbf{y} \in \mathbb{R}^p$ of system (6) has the form,

$$\mathbf{y} = \begin{bmatrix} \mathbf{C}_1 & \mathbf{C}_2 \end{bmatrix} \begin{bmatrix} \mathbf{x}_1 \\ \mathbf{x}_2 \end{bmatrix}. \quad (11)$$

Our objective is to design a regulator so that the output \mathbf{y} tracks a constant reference vector $\mathbf{r} \in \mathbb{R}^p$. We now introduce the vector variable \mathbf{x}_r , defined by the following differential equation,

$$\dot{\mathbf{x}}_r = \mathbf{r} - \mathbf{y}. \quad (12)$$

The controller should be designed in such a way so that

$$\lim_{t \rightarrow \infty} \dot{\mathbf{x}}_r(t) = \mathbf{0}.$$

To proceed, we define the augmented state variable vector,

$$\tilde{\mathbf{x}} = \begin{bmatrix} \mathbf{x}_r \\ \mathbf{x} \end{bmatrix} = \begin{bmatrix} \mathbf{x}_r \\ \overbrace{\begin{Bmatrix} \mathbf{x}_1 \\ \mathbf{x}_2 \end{Bmatrix}}^{\mathbf{x}} \end{bmatrix} \in \mathbb{R}^N, \quad (13)$$

where $N = n + p$. The dynamics of the overall augmented system are governed by the state equation,

$$\begin{bmatrix} \dot{\mathbf{x}}_r \\ \dot{\mathbf{x}}_1 \\ \dot{\mathbf{x}}_2 \end{bmatrix} = \underbrace{\begin{bmatrix} \mathbf{O} & -\mathbf{C}_1 & -\mathbf{C}_2 \\ \mathbf{O} & \mathbf{A}_{11} & \mathbf{A}_{12} \\ \mathbf{O} & \mathbf{A}_{21}(\mathbf{x}) & \mathbf{A}_{22}(\mathbf{x}) \end{bmatrix}}_{\tilde{\mathbf{A}}} \begin{bmatrix} \mathbf{x}_r \\ \mathbf{x}_1 \\ \mathbf{x}_2 \end{bmatrix} + \underbrace{\begin{bmatrix} \mathbf{I} \\ \mathbf{O} \\ \mathbf{O} \end{bmatrix}}_{\mathbf{B}_r} \mathbf{r} + \underbrace{\begin{bmatrix} \mathbf{O} \\ \mathbf{O} \\ \mathbf{B}_u \end{bmatrix}}_{\tilde{\mathbf{B}}} \mathbf{u}. \quad (14)$$

Note that the matrices in the augmented state equation (14) are labeled as $\tilde{\mathbf{A}}$, \mathbf{B}_r , and $\tilde{\mathbf{B}}$, respectively. Hence, the augmented system model (14) can be represented as

$$\dot{\tilde{\mathbf{x}}} = \tilde{\mathbf{A}} \tilde{\mathbf{x}} + \mathbf{B}_r \mathbf{r} + \tilde{\mathbf{B}} \mathbf{u}. \quad (15)$$

We make the following assumption:

Assumption 1: The pair

$$\left(\begin{bmatrix} \mathbf{O} & -\mathbf{C}_1 \\ \mathbf{O} & \mathbf{A}_{11} \end{bmatrix}, \begin{bmatrix} -\mathbf{C}_2 \mathbf{B}_u \\ \mathbf{A}_{12} \mathbf{B}_u \end{bmatrix} \right)$$

is controllable.

An essential element of the synergetic controller design is the construction of an invariant manifold $\boldsymbol{\sigma} = \mathbf{0}$. Let the manifold function $\boldsymbol{\sigma}$ be defined as

$$\boldsymbol{\sigma} = \boldsymbol{\sigma}(\tilde{\mathbf{x}}) = \boldsymbol{\sigma}(\mathbf{x}_r, \mathbf{x}_1, \mathbf{x}_2) = -\mathbf{S}_r \mathbf{x}_r + \mathbf{S}_1 \mathbf{x}_1 + \mathbf{S}_2 \mathbf{x}_2 = \begin{bmatrix} -\mathbf{S}_r & \mathbf{S}_1 & \mathbf{S}_2 \end{bmatrix} \tilde{\mathbf{x}} = \tilde{\mathbf{S}} \tilde{\mathbf{x}}. \quad (16)$$

The negative sign in front of \mathbf{S}_r is for the purpose of simplified notation. Proper construction of $\boldsymbol{\sigma}$ means that the system modeled by (14) restricted to the manifold $\mathcal{M} = \{\tilde{\mathbf{x}} : \boldsymbol{\sigma} = \mathbf{0}\}$ is asymptotically stable, that is, the trajectories of the system restricted to the manifold \mathcal{M} converge asymptotically toward the origin. A construction of such $\tilde{\mathbf{S}}$ is provided in the section. We assume that

$$\det(\tilde{\mathbf{S}} \tilde{\mathbf{B}}) = \det(\mathbf{S}_2 \mathbf{B}_u) \neq 0. \quad (17)$$

Using (3), we perform manipulations to obtain,

$$\begin{aligned} \mathbf{0} &= \mathbf{T} \dot{\boldsymbol{\sigma}} + \boldsymbol{\sigma} \\ &= \mathbf{T} \tilde{\mathbf{S}} \dot{\tilde{\mathbf{x}}} + \tilde{\mathbf{S}} \tilde{\mathbf{x}} \\ &= \mathbf{T} \tilde{\mathbf{S}} (\tilde{\mathbf{A}} \tilde{\mathbf{x}} + \mathbf{B}_r \mathbf{r} + \tilde{\mathbf{B}} \tilde{\mathbf{u}}) + \tilde{\mathbf{S}} \tilde{\mathbf{x}} \\ &= \mathbf{T} \tilde{\mathbf{S}} \tilde{\mathbf{A}} \tilde{\mathbf{x}} + \mathbf{T} \tilde{\mathbf{S}} \mathbf{B}_r \mathbf{r} + \mathbf{T} \tilde{\mathbf{S}} \tilde{\mathbf{B}} \tilde{\mathbf{u}} + \tilde{\mathbf{S}} \tilde{\mathbf{x}}. \end{aligned} \quad (18)$$

It follows from (14) that $\tilde{\mathbf{S}} \mathbf{B}_r = -\mathbf{S}_r$. Hence, we can re-write (18) as

$$\mathbf{0} = \mathbf{T} \tilde{\mathbf{S}} \tilde{\mathbf{A}} \tilde{\mathbf{x}} - \mathbf{T} \tilde{\mathbf{S}}_r \mathbf{r} + \mathbf{T} \tilde{\mathbf{S}} \tilde{\mathbf{B}} \tilde{\mathbf{u}} + \tilde{\mathbf{S}} \tilde{\mathbf{x}}. \quad (19)$$

Solving (19) for \mathbf{u} yields

$$\boxed{\tilde{\mathbf{u}} = -(\tilde{\mathbf{S}} \tilde{\mathbf{B}})^{-1} (\tilde{\mathbf{S}} \tilde{\mathbf{A}} \tilde{\mathbf{x}} + \mathbf{T}^{-1} \tilde{\mathbf{S}} \tilde{\mathbf{x}} - \mathbf{S}_r \mathbf{r})} \quad (20)$$

Substituting (20) into (14), we obtain closed-loop system dynamics model,

$$\dot{\tilde{\mathbf{x}}} = \left(\mathbf{I} - \tilde{\mathbf{B}} (\tilde{\mathbf{S}} \tilde{\mathbf{B}})^{-1} \tilde{\mathbf{S}} \right) \tilde{\mathbf{A}} \tilde{\mathbf{x}} - \tilde{\mathbf{B}} (\tilde{\mathbf{S}} \tilde{\mathbf{B}})^{-1} \mathbf{T}^{-1} \tilde{\mathbf{S}} \tilde{\mathbf{x}} + \tilde{\mathbf{B}} (\tilde{\mathbf{S}} \tilde{\mathbf{B}})^{-1} \mathbf{S}_r \mathbf{r} + \mathbf{B}_r \mathbf{r}. \quad (21)$$

In the following section, we show that the control law given by (20) forces the above closed-loop system to track the reference signal \mathbf{r} .

5 Analysis of the Closed-Loop System Behavior

To proceed with our analysis, we need the following lemma, which can be viewed as a corollary of Theorem 6.2 in [6, p. 333]; see also [10].

Lemma 1 *Consider the system model given by (14), where $\text{rank}(\tilde{\mathbf{B}}) = m$, Assumption 1 is satisfied, and a given set of $N - m$ complex numbers, $\{\lambda_1, \dots, \lambda_{N-m}\}$ is such that any λ_i whose imaginary part is nonzero appears in the above set in a conjugate pair. Then, there exist full-rank matrices $\mathbf{W} \in \mathbb{R}^{N \times (N-m)}$ and $\mathbf{W}^g \in \mathbb{R}^{(N-m) \times N}$ such that*

$$\mathbf{W}^g \mathbf{W} = \mathbf{I}_{N-m}, \quad \mathbf{W}^g \tilde{\mathbf{B}} = \mathbf{O},$$

and the eigenvalues of $\mathbf{W}^g \mathbf{A} \mathbf{W}$ are

$$\text{eig}(\mathbf{W}^g \tilde{\mathbf{A}} \mathbf{W}) = \{\lambda_1, \dots, \lambda_{N-m}\}.$$

Proof: We begin our proof by defining an $N \times (N - m)$ real matrix of the form,

$$\mathbf{V} = \begin{bmatrix} \mathbf{I}_{N-m} \\ \mathbf{O} \end{bmatrix}. \quad (22)$$

Therefore,

$$\begin{bmatrix} \mathbf{V} & \tilde{\mathbf{B}} \end{bmatrix}^{-1} = \begin{bmatrix} \mathbf{I}_{N-m} & \mathbf{O} \\ \mathbf{O} & \mathbf{B}_u \end{bmatrix}^{-1} = \begin{bmatrix} \mathbf{I}_{N-m} & \mathbf{O} \\ \mathbf{O} & \mathbf{B}_u^{-1} \end{bmatrix} = \begin{bmatrix} \mathbf{V}^g \\ \tilde{\mathbf{B}}^g \end{bmatrix}.$$

Hence,

$$\begin{bmatrix} \mathbf{V}^g \\ \tilde{\mathbf{B}}^g \end{bmatrix} \begin{bmatrix} \mathbf{V} & \tilde{\mathbf{B}} \end{bmatrix} = \begin{bmatrix} \mathbf{V}^g \mathbf{V} & \mathbf{V}^g \tilde{\mathbf{B}} \\ \tilde{\mathbf{B}}^g \mathbf{V} & \tilde{\mathbf{B}}^g \tilde{\mathbf{B}} \end{bmatrix} = \begin{bmatrix} \mathbf{I}_{N-m} & \mathbf{O} \\ \mathbf{O} & \mathbf{I}_m \end{bmatrix} = \mathbf{I}_N.$$

Note that

$$\mathbf{V}^g \mathbf{V} = \mathbf{I}_{N-m} \quad \text{and} \quad \mathbf{V}^g \tilde{\mathbf{B}} = \mathbf{O}. \quad (23)$$

By Assumptions 1, the pair

$$(\mathbf{V}^g \tilde{\mathbf{A}} \mathbf{V}, \mathbf{V}^g \tilde{\mathbf{A}} \tilde{\mathbf{B}}) = \left(\begin{bmatrix} \mathbf{O} & -\mathbf{C}_1 \\ \mathbf{O} & \mathbf{A}_{11} \end{bmatrix}, \quad \begin{bmatrix} -\mathbf{C}_2 \mathbf{B}_u \\ \mathbf{A}_{12} \mathbf{B}_u \end{bmatrix} \right)$$

is controllable. Therefore, for any set of complex numbers,

$$\{\lambda_1, \lambda_2, \dots, \lambda_{N-m}\}$$

symmetric with respect to the real axis, we can always find a matrix \mathbf{F} such that

$$\{\lambda_1, \lambda_2, \dots, \lambda_{N-m}\} = \text{eigenvalues} \left(\mathbf{V}^g \tilde{\mathbf{A}} \mathbf{V} - \mathbf{V}^g \tilde{\mathbf{A}} \tilde{\mathbf{B}} \mathbf{F} \right).$$

The matrix \mathbf{F} can be determined using any available method for pole placement. We proceed by performing the following manipulations,

$$\mathbf{V}^g \tilde{\mathbf{A}} \mathbf{V} - \mathbf{V}^g \tilde{\mathbf{A}} \tilde{\mathbf{B}} \mathbf{F} = \mathbf{V}^g \tilde{\mathbf{A}} \left(\mathbf{V} - \tilde{\mathbf{B}} \mathbf{F} \right) = \mathbf{W}^g \tilde{\mathbf{A}} \mathbf{W}, \quad (24)$$

where $\mathbf{W}^g = \mathbf{V}^g$ and $\mathbf{W} = \mathbf{V} - \tilde{\mathbf{B}} \mathbf{F}$. Note that by (23),

$$\mathbf{W}^g \mathbf{W} = \mathbf{V}^g \left(\mathbf{V} - \tilde{\mathbf{B}} \mathbf{F} \right) = \mathbf{V}^g \mathbf{V} = \mathbf{I}_{N-m}. \quad (25)$$

We also have, $\mathbf{V}^g \tilde{\mathbf{B}} = \mathbf{W}^g \tilde{\mathbf{B}} = \mathbf{O}$, which completes the proof of the lemma. \square

Theorem 2 Suppose that the assumptions of Lemma 1 are satisfied. Then there exists the invariant manifold matrix $\tilde{\mathbf{S}} \in \mathbb{R}^{m \times N}$ such that $\tilde{\mathbf{S}} \tilde{\mathbf{B}} = \mathbf{I}_m$ and the closed-loop system (21) tracks the reference signal \mathbf{r} , that is, $\mathbf{y}(\infty) = \mathbf{r}$.

Proof: Consider the matrix, $\begin{bmatrix} \mathbf{W} & \tilde{\mathbf{B}} \end{bmatrix}$. Note that

$$\begin{bmatrix} \mathbf{W} & \tilde{\mathbf{B}} \end{bmatrix} = \begin{bmatrix} \mathbf{I}_{N-m} & \mathbf{O} \\ \mathbf{F} & \mathbf{I}_m \end{bmatrix} \begin{bmatrix} \mathbf{V}^g \\ \tilde{\mathbf{B}}^g \end{bmatrix}.$$

Thus the matrix $\begin{bmatrix} \mathbf{W} & \tilde{\mathbf{B}} \end{bmatrix}$ is invertible and its inverse has the form

$$\begin{bmatrix} \mathbf{W} & \tilde{\mathbf{B}} \end{bmatrix}^{-1} = \begin{bmatrix} \mathbf{W}^g \\ \tilde{\mathbf{B}}^g + \mathbf{F} \mathbf{V}^g \end{bmatrix}.$$

Let

$$\tilde{\mathbf{S}} = \tilde{\mathbf{B}}^g + \mathbf{F} \mathbf{V}^g = \begin{bmatrix} \mathbf{F} & \mathbf{B}_u^{-1} \end{bmatrix}.$$

Note that by (23),

$$\tilde{\mathbf{S}}\tilde{\mathbf{B}} = \left(\tilde{\mathbf{B}}^g + \mathbf{F}\mathbf{V}^g \right) \tilde{\mathbf{B}} = \mathbf{I}_m.$$

Consider the following state-space transformation,

$$\mathbf{z} = \begin{bmatrix} \mathbf{z}_1 \\ \mathbf{z}_2 \end{bmatrix} = \begin{bmatrix} \mathbf{W}^g \\ \tilde{\mathbf{S}} \end{bmatrix} \tilde{\mathbf{x}} = \begin{bmatrix} \mathbf{V}^g \\ \tilde{\mathbf{S}} \end{bmatrix} \tilde{\mathbf{x}}.$$

Note that $\mathbf{z}_2 = \tilde{\mathbf{S}}\tilde{\mathbf{x}} = \boldsymbol{\sigma}$. We also have

$$\begin{bmatrix} \mathbf{W}^g \\ \tilde{\mathbf{S}} \end{bmatrix} \begin{bmatrix} \mathbf{W} & \tilde{\mathbf{B}} \end{bmatrix} = \begin{bmatrix} \mathbf{W}^g\mathbf{W} & \mathbf{W}^g\tilde{\mathbf{B}} \\ \tilde{\mathbf{S}}\mathbf{W} & \tilde{\mathbf{S}}\tilde{\mathbf{B}} \end{bmatrix} = \begin{bmatrix} \mathbf{I}_{N-m} & \mathbf{O} \\ \mathbf{O} & \mathbf{I}_m \end{bmatrix}, \quad (26)$$

where \mathbf{I}_{N-m} is the identity matrix of dimension $(N-m) \times (N-m)$. Therefore, the matrices in (26) satisfy the following relations,

$$\left. \begin{aligned} \mathbf{W}^g\mathbf{W} &= \mathbf{I}_{N-m}, & \mathbf{W}^g\tilde{\mathbf{B}} &= \mathbf{O} \in \mathbb{R}^{(N-m) \times m}, \\ \tilde{\mathbf{S}}\mathbf{W} &= \mathbf{O} \in \mathbb{R}^{m \times (N-m)}, & \tilde{\mathbf{S}}\tilde{\mathbf{B}} &= \mathbf{I}_m. \end{aligned} \right\} \quad (27)$$

Using matrix relations shown in (27), we represent the closed-loop dynamics in the \mathbf{z} coordinates as

$$\begin{aligned} \begin{bmatrix} \dot{\mathbf{z}}_1 \\ \dot{\mathbf{z}}_2 \end{bmatrix} &= \begin{bmatrix} \mathbf{W}^g \\ \tilde{\mathbf{S}} \end{bmatrix} (\tilde{\mathbf{A}} - \tilde{\mathbf{B}}(\tilde{\mathbf{S}}\tilde{\mathbf{B}})^{-1}\tilde{\mathbf{S}}\tilde{\mathbf{A}} - \tilde{\mathbf{B}}(\tilde{\mathbf{S}}\tilde{\mathbf{B}})^{-1}\mathbf{T}^{-1}\tilde{\mathbf{S}}) \begin{bmatrix} \mathbf{W} & \tilde{\mathbf{B}} \end{bmatrix} \begin{bmatrix} \mathbf{z}_1 \\ \mathbf{z}_2 \end{bmatrix} \\ &\quad - \begin{bmatrix} \mathbf{W}^g \\ \tilde{\mathbf{S}} \end{bmatrix} \tilde{\mathbf{B}}(\tilde{\mathbf{S}}\tilde{\mathbf{B}})^{-1}\tilde{\mathbf{S}}\mathbf{B}_r \mathbf{r} + \begin{bmatrix} \mathbf{W}^g \\ \tilde{\mathbf{S}} \end{bmatrix} \mathbf{B}_r \mathbf{r} \\ &= \begin{bmatrix} \mathbf{W}^g\tilde{\mathbf{A}}\mathbf{W} & \mathbf{W}^g\tilde{\mathbf{A}}\tilde{\mathbf{B}} \\ \mathbf{O} & -\mathbf{T}^{-1} \end{bmatrix} \begin{bmatrix} \mathbf{z}_1 \\ \mathbf{z}_2 \end{bmatrix} + \begin{bmatrix} \mathbf{W}^g \\ \tilde{\mathbf{S}} \end{bmatrix} (-\tilde{\mathbf{B}}(\tilde{\mathbf{S}}\tilde{\mathbf{B}})^{-1}\tilde{\mathbf{S}}\mathbf{B}_r + \mathbf{B}_r) \mathbf{r} \\ &= \begin{bmatrix} \mathbf{W}^g\tilde{\mathbf{A}}\mathbf{W} & \mathbf{W}^g\tilde{\mathbf{A}}\tilde{\mathbf{B}} \\ \mathbf{O} & -\mathbf{T}^{-1} \end{bmatrix} \begin{bmatrix} \mathbf{z}_1 \\ \mathbf{z}_2 \end{bmatrix} + \begin{bmatrix} \mathbf{O} + \mathbf{W}^g\mathbf{B}_r \\ -\tilde{\mathbf{S}}\mathbf{B}_r + \tilde{\mathbf{S}}\mathbf{B}_r \end{bmatrix} \mathbf{r} \\ &= \begin{bmatrix} \mathbf{W}^g\tilde{\mathbf{A}}\mathbf{W} & \mathbf{W}^g\tilde{\mathbf{A}}\tilde{\mathbf{B}} \\ \mathbf{O} & -\mathbf{T}^{-1} \end{bmatrix} \begin{bmatrix} \mathbf{z}_1 \\ \mathbf{z}_2 \end{bmatrix} + \begin{bmatrix} \mathbf{W}^g\mathbf{B}_r \\ \mathbf{O} \end{bmatrix} \mathbf{r}. \end{aligned} \quad (28)$$

Observe that $\mathbf{W}^g\tilde{\mathbf{B}}(\tilde{\mathbf{S}}\tilde{\mathbf{B}})^{-1}\tilde{\mathbf{S}}\mathbf{B}_r = \mathbf{O}$ because $\mathbf{W}^g\tilde{\mathbf{B}} = \mathbf{O}$. Since \mathbf{T} is positive definite, the eigenvalues of $-\mathbf{T}^{-1}$ are all in the open left-hand complex plane. This implies that the

dynamics of $\mathbf{z}_2 = \boldsymbol{\sigma}$ are asymptotically stable, that is, the invariant manifold, $\{\boldsymbol{\sigma} = \mathbf{0}\}$, is asymptotically attractive. By (24), the matrix \mathbf{W} can be chosen so that the eigenvalues of the constant matrix $\mathbf{W}^g \tilde{\mathbf{A}} \mathbf{W}$ are in the open left-hand complex plane. In the steady-state the overall system trajectories converge to the point on the manifold, $\{\mathbf{z}_2 = \boldsymbol{\sigma} = \mathbf{0}\}$, given by

$$\mathbf{0} = \mathbf{W}^g \tilde{\mathbf{A}} \mathbf{W} \mathbf{z}_1 + \mathbf{W}^g \mathbf{B}_r \mathbf{r}. \quad (29)$$

We partition \mathbf{F} as

$$\mathbf{F} = \begin{bmatrix} \mathbf{F}_1 & \mathbf{F}_2 \end{bmatrix}, \quad (30)$$

where $\mathbf{F}_1 \in \mathbb{R}^{m \times p}$ and $\mathbf{F}_2 \in \mathbb{R}^{m \times (n-m)}$. We have,

$$\mathbf{W} = \mathbf{V} - \tilde{\mathbf{B}} \mathbf{F} = \begin{bmatrix} \mathbf{I}_p & \mathbf{O} \\ \mathbf{O} & \mathbf{I}_{n-m} \\ -\mathbf{B}_u \mathbf{F}_1 & -\mathbf{B}_u \mathbf{F}_1 \end{bmatrix} \quad \text{and} \quad \mathbf{W}^g \mathbf{B}_r = \begin{bmatrix} \mathbf{I}_p \\ \mathbf{O}_{(n-m) \times p} \end{bmatrix}. \quad (31)$$

Recall that $\mathbf{W}^g = \mathbf{V}^g$. Using the above and the fact that

$$\mathbf{z}_1 = \mathbf{W}^g \tilde{\mathbf{x}} = \begin{bmatrix} \mathbf{x}_r \\ \mathbf{x}_1 \end{bmatrix},$$

we express (29) in the form,

$$\begin{aligned} \mathbf{0} &= \mathbf{V}^g \begin{bmatrix} \mathbf{O} & -\mathbf{C}_1 & -\mathbf{C}_2 \\ \mathbf{O} & \mathbf{A}_{11} & \mathbf{A}_{12} \\ \mathbf{O} & \mathbf{A}_{21}(\mathbf{x}) & \mathbf{A}_{22}(\mathbf{x}) \end{bmatrix} \mathbf{W} \mathbf{z}_1 + \begin{bmatrix} \mathbf{I}_p \\ \mathbf{O} \end{bmatrix} \mathbf{r} \\ &= \begin{bmatrix} \mathbf{C}_2 \mathbf{B}_u \mathbf{F}_1 & -\mathbf{C}_1 + \mathbf{C}_2 \mathbf{B}_u \mathbf{F}_2 \\ -\mathbf{A}_{12} \mathbf{B}_u \mathbf{F}_1 & \mathbf{A}_{11} - \mathbf{A}_{12} \mathbf{B}_u \mathbf{F}_2 \end{bmatrix} \mathbf{W}^g \tilde{\mathbf{x}} + \begin{bmatrix} \mathbf{I}_p \\ \mathbf{O} \end{bmatrix} \mathbf{r} \\ &= \begin{bmatrix} \mathbf{C}_2 \mathbf{B}_u \mathbf{F}_1 & -\mathbf{C}_1 + \mathbf{C}_2 \mathbf{B}_u \mathbf{F}_2 \\ -\mathbf{A}_{12} \mathbf{B}_u \mathbf{F}_1 & \mathbf{A}_{11} - \mathbf{A}_{12} \mathbf{B}_u \mathbf{F}_2 \end{bmatrix} \begin{bmatrix} \mathbf{x}_r \\ \mathbf{x}_1 \end{bmatrix} + \begin{bmatrix} \mathbf{I}_p \\ \mathbf{O} \end{bmatrix} \mathbf{r}, \end{aligned}$$

or, equivalently,

$$\mathbf{0} = \mathbf{C}_2 \mathbf{B}_u \mathbf{F}_1 \mathbf{x}_r - (\mathbf{C}_1 - \mathbf{C}_2 \mathbf{B}_u \mathbf{F}_2) \mathbf{x}_1 + \mathbf{r}, \quad (32)$$

$$\mathbf{0} = -\mathbf{A}_{12} \mathbf{B}_u \mathbf{F}_1 \mathbf{x}_r + (\mathbf{A}_{11} - \mathbf{A}_{12} \mathbf{B}_u \mathbf{F}_2) \mathbf{x}_1. \quad (33)$$

In the steady-state, $\mathbf{z}_2 = \mathbf{0}$, that is,

$$\tilde{\mathbf{S}}\tilde{\mathbf{x}} = \begin{bmatrix} -S_r & S_1 & S_2 \end{bmatrix} \begin{bmatrix} \mathbf{x}_r \\ \mathbf{x}_1 \\ \mathbf{x}_2 \end{bmatrix} = \mathbf{0}.$$

Hence,

$$\mathbf{S}_r \mathbf{x}_r = \mathbf{S}_1 \mathbf{x}_1 + \mathbf{S}_2 \mathbf{x}_2. \quad (34)$$

Substituting $\mathbf{S}_2 = \mathbf{B}_u^{-1}$ and (34) into (32), we obtain

$$\begin{aligned} \mathbf{0} &= -\mathbf{C}_2 \mathbf{B}_u \mathbf{S}_r \mathbf{x}_r - \mathbf{C}_1 \mathbf{x}_1 + \mathbf{C}_2 \mathbf{B}_u \mathbf{S}_1 \mathbf{x}_1 + \mathbf{r} \\ &= \mathbf{C}_2 \mathbf{B}_u (-\mathbf{S}_1 \mathbf{x}_1 - \mathbf{S}_2 \mathbf{x}_2) - \mathbf{C}_1 \mathbf{x}_1 + \mathbf{C}_2 \mathbf{B}_u \mathbf{S}_1 \mathbf{x}_1 + \mathbf{r} \\ &= -\mathbf{C}_2 \mathbf{x}_2 - \mathbf{C}_1 \mathbf{x}_1 + \mathbf{r} \\ &= -\mathbf{y} + \mathbf{r}, \end{aligned}$$

that is, $\mathbf{y}(\infty) = \mathbf{r}$, which completes the proof of the theorem. \square

We summarize the above considerations in the form of an algorithm for constructing a matrix $\tilde{\mathbf{S}}$ of the invariant manifold.

Algorithm for the Construction of an Invariant Manifold

1. Find a matrix \mathbf{V} such that $\begin{bmatrix} \mathbf{V} & \tilde{\mathbf{B}} \end{bmatrix}$ is invertible.
2. The first $(N - m)$ rows of $\begin{bmatrix} \mathbf{V} & \tilde{\mathbf{B}} \end{bmatrix}^{-1}$ form the matrix \mathbf{V}^g , that is,

$$\begin{bmatrix} \mathbf{V} & \tilde{\mathbf{B}} \end{bmatrix}^{-1} = \begin{bmatrix} \mathbf{V}^g \\ \tilde{\mathbf{B}}^g \end{bmatrix}.$$

3. Check if the pair $(\mathbf{V}^g \tilde{\mathbf{A}} \mathbf{V}, \mathbf{V}^g \tilde{\mathbf{A}} \tilde{\mathbf{B}})$ is controllable. If yes, construct a gain matrix \mathbf{F} such that the eigenvalues of the matrix

$$\mathbf{V}^g \tilde{\mathbf{A}} \mathbf{V} - \mathbf{V}^g \tilde{\mathbf{A}} \tilde{\mathbf{B}} \mathbf{F}$$

are in desired locations.

4. Construct the matrix $\tilde{\mathbf{S}}$ using the relation,

$$\tilde{\mathbf{S}} = \tilde{\mathbf{B}}^g + \mathbf{F}\mathbf{V}^g = \begin{bmatrix} \mathbf{F} & \mathbf{B}_u^{-1} \end{bmatrix}.$$

6 Examples

6.1 Roll-trajectory following in wing-rock suppression system

To illustrate the use of the integral synergetic control for trajectory tracking, we consider the following nonlinear wing-rock dynamics [11],

$$\ddot{\phi} = \alpha_1\phi + \alpha_2\dot{\phi} + \alpha_3\dot{\phi}^2 + \alpha_4\phi^2\dot{\phi} + \alpha_5\dot{\phi}^2\phi + bu, \quad (35)$$

where ϕ is the aircraft roll-angle, in degrees, and u is the control input. The parameters for this system are: $\alpha_1 = -0.0148927$, $\alpha_2 = 0.0415424$, $\alpha_3 = 0.01668756$, $\alpha_4 = -0.06578382$, $\alpha_5 = 0.08578836$, and $b = 0.100$. The control objective is to suppress sustained limit-cycle oscillations induced by the wing-rock. We construct a synergetic controller so that the angle ϕ follows a piecewise constant reference signal profile. Let $x_1 = \phi$, $x_2 = \dot{\phi}$, and let $\dot{x}_r = r - x_1$, where $r = \phi_r$ is the reference, $y = x_1$ is the output. Using the above notation, we combine the plant model and the reference dynamics to obtain the following augmented model,

$$\begin{bmatrix} \dot{x}_r \\ \dot{x}_1 \\ \dot{x}_2 \end{bmatrix} = \underbrace{\begin{bmatrix} 0 & -1 & 0 \\ 0 & 0 & 1 \\ 0 & \alpha_1 + \alpha_5 x_2^2 & \alpha_2 + \alpha_3 x_2 + \alpha_4 x_1^2 \end{bmatrix}}_{\tilde{\mathbf{A}}} \underbrace{\begin{bmatrix} x_r \\ x_1 \\ x_2 \end{bmatrix}}_{\tilde{\mathbf{x}}} + \begin{bmatrix} 1 \\ 0 \\ 0 \end{bmatrix} r + \underbrace{\begin{bmatrix} 0 \\ 0 \\ b \end{bmatrix}}_{\tilde{\mathbf{B}}} u. \quad (36)$$

It is easy to verify that

$$\dot{\tilde{\mathbf{x}}} = \begin{bmatrix} r - x_1 \\ x_2 \\ \alpha_1 x_1 + \alpha_5 x_2^2 x_1 + \alpha_2 x_2 + \alpha_3 x_2^2 + \alpha_4 x_1^2 x_2 + bu \end{bmatrix}.$$

We then employ the algorithm described above to construct an attractive invariant manifold. We begin by selecting

$$\mathbf{V} = \begin{bmatrix} 1 & 0 \\ 0 & 1 \\ 0 & 0 \end{bmatrix} \quad \text{and} \quad \mathbf{F} = \begin{bmatrix} -0.75 & 2.00 \end{bmatrix}$$

to place the eigenvalues of $\mathbf{V}^g \tilde{\mathbf{A}}\mathbf{V} - \mathbf{V}^g \tilde{\mathbf{A}}\tilde{\mathbf{B}}\mathbf{F}$ at -0.5 and -1.5 . Performing manipulations described in the algorithm, we obtain the manifold

$$\boldsymbol{\sigma} = \begin{bmatrix} -\frac{1}{2b} & \frac{3}{2b} & \frac{1}{b} \end{bmatrix} \tilde{\mathbf{x}} = \tilde{\mathbf{S}}\tilde{\mathbf{x}} = \mathbf{0}. \quad (37)$$

The synergetic control law has the form,

$$\mathbf{u}(\tilde{\mathbf{x}}) = -(\tilde{\mathbf{S}}\tilde{\mathbf{B}})^{-1} \left(\tilde{\mathbf{S}}\tilde{\mathbf{A}}\tilde{\mathbf{x}} + \tilde{\mathbf{S}}\mathbf{B}_r r + \mathbf{T}^{-1}\tilde{\mathbf{S}} \right) \tilde{\mathbf{x}}. \quad (38)$$

The resulting closed loop dynamics are described by

$$\begin{bmatrix} \dot{\mathbf{z}}_1 \\ \dot{\mathbf{z}}_2 \end{bmatrix} = \left[\begin{array}{cc|c} 0 & -1 & 0 \\ 0.5 & -1.5 & b \\ \hline 0 & 0 & -\mathbf{T}^{-1} \end{array} \right] \begin{bmatrix} \mathbf{z}_1 \\ \mathbf{z}_2 \end{bmatrix} + \begin{bmatrix} 1 \\ 0 \\ 0 \end{bmatrix} r,$$

where $\mathbf{z}_1 = [x_r \ x_1]^\top$, $\mathbf{z}_2 = \boldsymbol{\sigma}$. Note that the eigenvalues of the closed loop dynamics are -0.5 , -1.5 , and $-\mathbf{T}^{-1}$, which guarantee that the tracking error converges to zero, that is, at steady-state, $x_1 = r$. In this example, we use $\mathbf{T} = 1$. To see this, at steady-state, we have

$$\begin{bmatrix} 0 \\ 0 \end{bmatrix} = \left[\begin{array}{cc} 0 & -1 \\ 0.5 & -1.5 \end{array} \right] \begin{bmatrix} x_r \\ x_1 \end{bmatrix} + \begin{bmatrix} 1 \\ 0 \end{bmatrix} r.$$

Solving the above matrix equation for x_r and x_1 , we obtain $x_r = 3r$ and $x_1 = r$. Therefore, at steady-state $x_1 = r$.

We present simulation results illustrating the performance of integral synergetic controller in Figures 1 and 2. We show in Figure 1 trajectories of (36) driven by the control strategy (38) where solid lines represent $x_1(t)$, dotted lines represent $x_2(t)$, and dashed-lines represent $\phi_r(t)$. We can see that as the transient become negligible, $x_1(t)$ closely tracks $\phi_r(t)$.

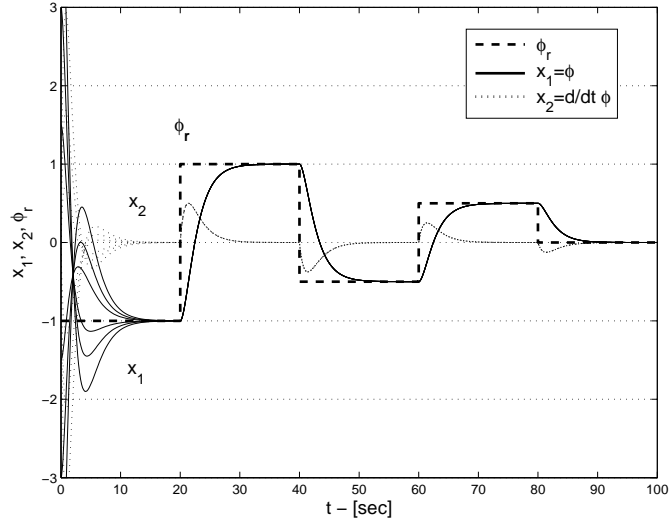


Figure 1: The roll angle $\phi(t)$, denoted $x_1(t)$, tracking reference angle $\phi_r(t)$: several plots for different initial conditions.

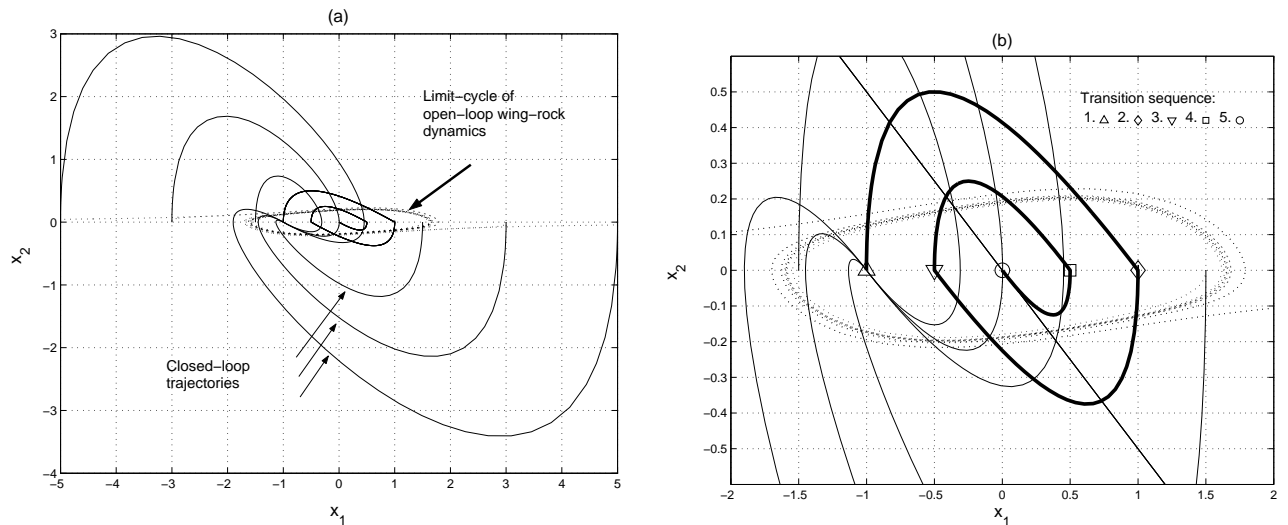


Figure 2: Phase trajectories of the closed-loop system driven by the integral synergetic controller originating from several initial conditions: (a) general view, (b) magnified view.

In Figure 2, we show phase portraits of nonlinear wing-rock dynamics. In Figure 2(a), dotted lines indicate sustained limit-cycle oscillations of the uncompensated closed-loop system. Thick solid lines denote the closed-loop phase trajectories emanating from different initial conditions of the closed-loop system driven by the synergetic controller. In Figure 2(b), we show a magnified portion of the phase portrait in the neighborhood of the origin from Figure 2(a). The solid line indicates transitions from several constant reference values, denoted by the sequence of symbols: \triangle , \diamond , ∇ , \square (see these values from Fig. 1) towards the ultimate destination: the origin, denoted by the symbol \odot .

6.2 Two-link robotic manipulator

We now synthesize a regulator for the two-link robotic manipulator depicted in Figure 3. We first concern ourselves with constructing a mathematical model. The Lagrangian has the form,

$$\begin{aligned} L = & \frac{1}{2}m_1l_1^2\omega_1^2 + \frac{1}{2}m_2(l_1^2\omega_1^2 + l_2^2\omega_2^2 + 2l_1l_2\cos(\theta_2 - \theta_1)\omega_1\omega_2) \\ & + m_1gl_1\cos(\theta_1) + m_2g(l_1\cos(\theta_1) + l_2\cos(\theta_2)), \end{aligned}$$

where $\omega_i = \dot{\theta}_i$, $i = 1, 2$, are the angular velocities of the links, and m_i and l_i are the link masses and their lengths, respectively. We assume that the input torques, τ_1 and τ_2 are applied at each joint. The parameter values are given in Table 1. We next write the

Table 1: Parameter numerical values of the two-link robotic manipulator.

$m_1 = m_2$	1 kg
$l_1 = l_2$	0.5 m
g	9.81 m/sec ²

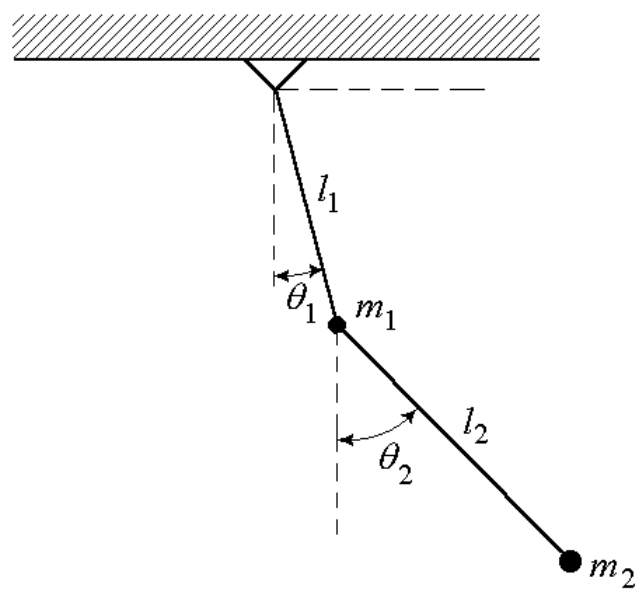


Figure 3: A two-link robotic manipulator.

Lagrange equations of motion for the system,

$$\begin{bmatrix} (m_1 + m_2)l_1^2 & m_2l_1l_2 \cos(\theta_2 - \theta_1) \\ m_2l_1l_2 \cos(\theta_2 - \theta_1) & m_2l_2^2 \end{bmatrix} \begin{bmatrix} \ddot{\theta}_1 \\ \ddot{\theta}_2 \end{bmatrix} = \begin{bmatrix} \tau_1 - \tau_2 + m_2l_1l_2\dot{\theta}_2^2 \sin(\theta_2 - \theta_1) - (m_1 + m_2)gl_1 \sin(\theta_1) \\ \tau_2 - m_2l_1l_2\dot{\theta}_1^2 \sin(\theta_2 - \theta_1) - m_2gl_2 \sin(\theta_2) \end{bmatrix}. \quad (39)$$

Note that the manipulator inertia matrix, \mathbf{H} , on the left-hand side of the above equation is symmetric and positive definite, and its determinant is

$$\det \mathbf{H} = (m_1 + m_2)m_2l_1^2l_2^2 - m_2^2l_1^2l_2^2 \cos^2(\theta_2 - \theta_1) > 0.$$

We represent the above model in state-space format, where the state variables are defined as, $x_1 = \theta_1$, $x_2 = \theta_2$, $x_3 = \dot{\theta}_1$, and $x_4 = \dot{\theta}_2$. First, using the above notation, we represent (39) as

$$\mathbf{H}(\mathbf{x}_1)\ddot{\mathbf{x}}_1 = -\mathbf{C}(\mathbf{x}_1, \dot{\mathbf{x}}_1)\dot{\mathbf{x}}_1 - \mathbf{g}(\mathbf{x}_1) + \mathbf{B}_u\boldsymbol{\tau},$$

where

$$\mathbf{B}_u = \begin{bmatrix} 1 & -1 \\ 0 & 1 \end{bmatrix},$$

and

$$\mathbf{g}(\mathbf{x}_1) = \mathbf{G}(\mathbf{x}_1)\mathbf{x}_1 = \begin{bmatrix} -(m_1 + m_2)gl_1 \frac{\sin(x_1)}{x_1} & 0 \\ 0 & -m_2gl_2 \frac{\sin(x_2)}{x_2} \end{bmatrix} \mathbf{x}_1.$$

With the above notation in place we represent as in (10), where

$$\tilde{\mathbf{u}} = \mathbf{H}^{-1}\mathbf{B}_u\boldsymbol{\tau}.$$

We select

$$\mathbf{T} = 0.05\mathbf{I}_2,$$

and

$$\{\lambda_1, \lambda_2, \lambda_3, \lambda_4\} = \{-3, -3.5, -4, -4.5\}.$$

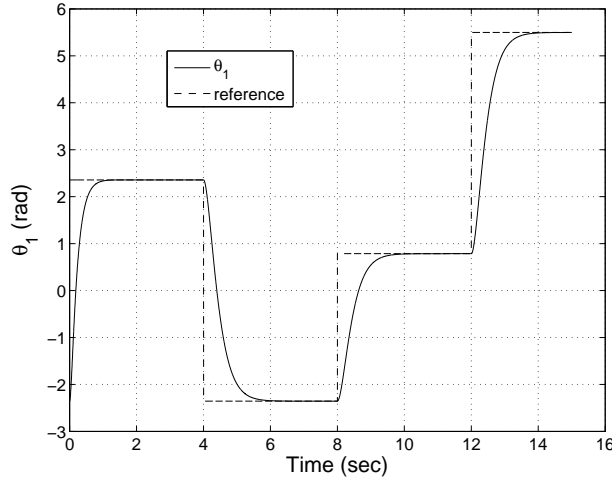


Figure 4: A plot of θ_1 and its reference versus time.

Applying the design algorithm, we obtain

$$\tilde{\mathbf{S}} = \begin{bmatrix} -18. & 0 & 8.5 & 0 & 1 & 0 \\ 0 & -10.5 & 0 & 6.5 & 0 & 1 \end{bmatrix}.$$

With the above data, we construct the synergetic regulator (20). In our simulations, we select the initial conditions to be,

$$\mathbf{x}_r(0) = \mathbf{0} \quad \text{and} \quad \mathbf{x}(0)^\top = \begin{bmatrix} -3/4\pi & \pi & 0 & 0 \end{bmatrix}.$$

The components of the reference signal vector \mathbf{r} are plotted in Figures 4 and 5, where we show plots of link angles θ_1 and θ_2 versus time. In Figures 6 and 7, we show plots of the time history of the x and y coordinates, respectively, of the end effector of the robotic manipulator. In Figure 8, we plot the path of the end effector in the (x, y) plane. As can be seen from the Figures the reference signal is tracked as predicted by the theory.

7 Conclusions

We presented a regulator design algorithm for nonlinear dynamical systems using integral synergetic control. The solution to the above nonlinear regulator problem is derived for a

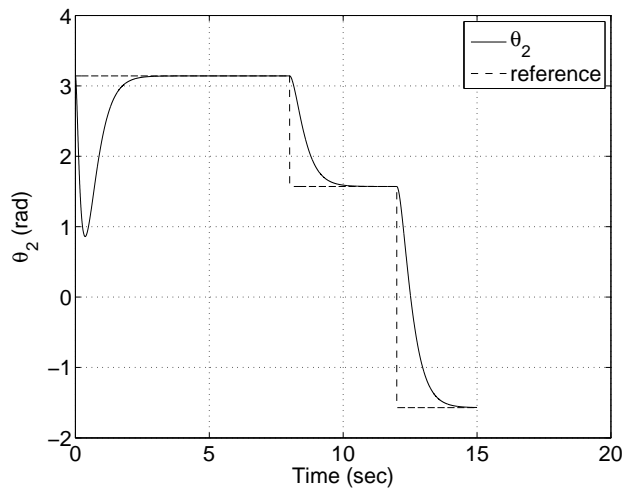


Figure 5: A plot of θ_2 and its reference versus time.

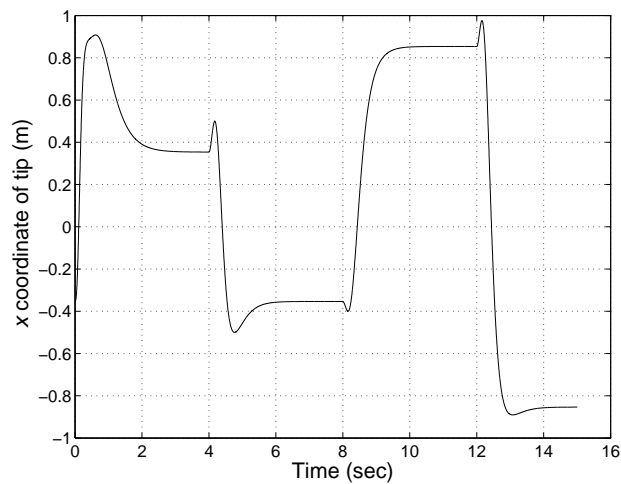


Figure 6: A plot of the x -coordinate of the end effector versus time.

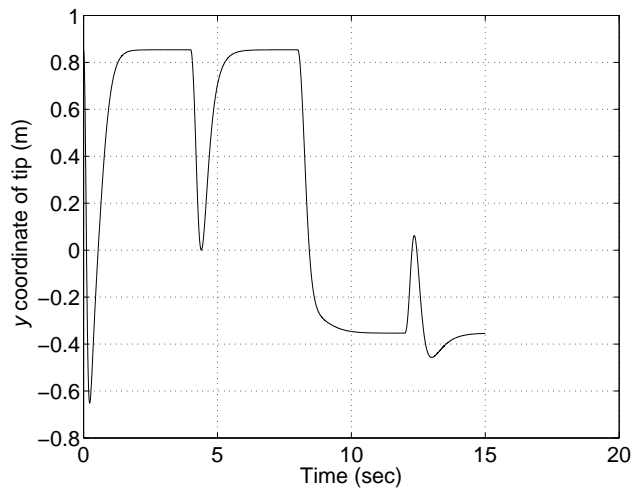


Figure 7: A plot of the y -coordinate of the end effector versus time.

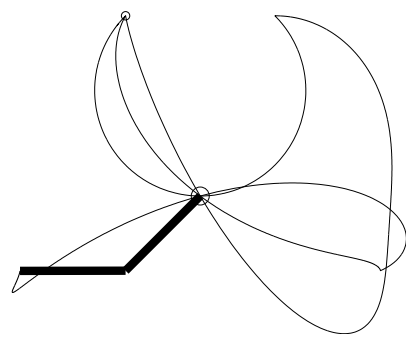


Figure 8: A plot of the path of the end effector in the (x, y) -plane.

class of nonlinear systems in the “regular form” with nonlinearities satisfying the matching condition using a synergetic control approach.

The proposed synergetic regulator design methodology incorporates an additional state vector representing the integral of the tracking error. The construction of an asymptotically stable invariant manifold uses the augmented state vector in order to drive the integral of the tracking error to zero. Using the augmented state vector, we convert the initial tracking problem into the equivalent regulation problem for which we can readily apply the synergetic control design methodology.

This design methodology consists of two steps: the manifold design and the control law design. An algorithm is presented for the construction of an asymptotically stable invariant manifold in such a way that all trajectories confined to the manifold converge to the origin. Once a manifold is constructed, the synergetic control strategy can be easily obtained by solving the first-order differential equation of regulated variables. Finally, the proposed design procedure is illustrated on a nonlinear wing-rock suppression problem and a two-link robotic manipulator. Simulations show that integral synergetic regulator yields an excellent tracking performance.

References

- [1] E. Santi, A. Monti, D. Li, K. Proddutur, and R. Dougal, “Synergetic control for DC-DC boost converter: Implementation options,” *IEEE Transactions on Industry Applications*, vol. 39, no. 6, pp. 1803–1813, November/December 2003.
- [2] ——, “Synergetic Control for Power Electronics Applications: A Comparison with the Sliding Mode Approach,” *Journal of Circuits, Systems, and Computers*, vol. 13, no. 4, pp. 737–760, 2004.
- [3] Nusawardhana and S. H. Žak, “Optimality of synergetic controllers,” in *Proceedings of 2006 ASME International Mechanical Engineering Congress and Exposition*, American Society of Mechanical Engineers. Chicago, IL: ASME, November 5–10 2006.

- [4] Nusawardhana, S. H. Žak, and W. A. Crossley, “Nonlinear synergetic optimal control,” *AIAA Journal of Guidance, Control, and Dynamics*, vol. Vol. 30, no. No. 4, pp. 1134–1147, JulyAugust 2007.
- [5] A. B. Açıkmese and M. Corless, “Robust Output Tracking for Uncertain/Nonlinear Systems Subject to Almost Constant Disturbances,” *Automatica*, vol. 38, pp. 1919–1926, 2002.
- [6] S. H. Žak, *Systems and Control*. New York: Oxford University Press, 2003.
- [7] C. Edwards and S. Spurgeon, *Sliding Mode Control: Theory and Applications*. Taylor & Francis, 1998.
- [8] V. Utkin, *Sliding Modes in Control and Optimization*. Heidelberg: Springer-Verlag Berlin, 1992.
- [9] J. Slotine and W. Li, *Applied Nonlinear Control*. Englewood Cliffs, NJ: Prentice Hall, Inc., 1991.
- [10] S. H. Žak and S. Hui, “On variable structure output feedback controllers of uncertain dynamic systems,” *IEEE Transactions on Automatic Control*, vol. 38, no. 10, pp. 1509–1512, October 1993.
- [11] K. Passino, *Biomimicry for Optimization, Control, and Automation*. London, UK: Springer-Verlag, 2005.